Insights into the wettability transition of nanosecond laser ablated surface under ambient air exposure

Zhen Yang [a,b] , Xianping Liu [b], Yanling Tian [a,b,*]

[a]School of Mechanical Engineering, Tianjin University, Tianjin 300350, China

[b]School of Engineering, University of Warwick, Coventry CV4 7AL, UK

*Corresponding author e-mail address: meytian@tju.edu.cn

Abstract

Super-hydrophobic surfaces are attractive due to self-cleaning and anti-corrosive behaviors in harsh environments. Laser texturing offers a facile method to produce super-hydrophobic surfaces. However, the results indicated that the fresh laser ablated surface was generally super-hydrophilic and then gradually reached super-hydrophobic state when exposed to ambient air for certain time. Investigating wettability changing mechanism could contribute to reducing wettability transition period and improving industrial productivity. To solve this problem, we have studied the bare aluminum surface, fresh laser ablated super-hydrophilic surface, 15-day air exposed surface, and the aged super-hydrophobic surface by time-dependent water contact angle (WCA) and rolling angle (RA), scanning electron microscopy (SEM), 3D profile and X-ray photoelectron spectroscopy (XPS). The origins of super-hydrophilicity of the fresh laser ablated surface are identified as (1) the formation of hierarchical rough structures and (2) the surface chemical modifications (the decrease of nonpolar carbon, the formation of hydrophilic alumina and residual unsaturated atoms). The chemisorbed nonpolar airborne hydrocarbons from air moisture contributed to the gradual super-hydrophobic transition, which can be proved by the thermal annealing experiment. Particularly, to clearly explore the wettability transition mechanism, we extensively discussed why the laser-induced freshly outer layer was super-hydrophilic and how the airborne hydrocarbons were chemisorbed. This work not only provides useful insights into the formation mechanism of laser ablated super-hydrophobic surfaces, but also further guides industry to effectively modify surface chemistry to reduce wettability transition period and rapidly produce stable and durable super-hydrophobic surfaces.

Keywords: Nanosecond laser, Wettability transition, Surface morphology, Airborne hydrocarbons, Thermal annealing

1. Introduction

Super-hydrophobic surfaces have promising prospects in the areas including self-cleaning [1], drag reduction [2], anti-corrosion [3] and enhanced heat transfer [4]. When a droplet beads up with water contact angle (WCA) over 150°, the solid surface is defined as super-hydrophobic with the lotus effect (i.e., rolling angle (RA) less than 10°) or the pinning effect (i.e., no RA or RA greater than 10°) [5]. Many approaches have been developed for the fabrication of super-hydrophobic surfaces, such as thermal embossing [6], sol-gel [7], chemical etching [8], electrodeposition [9] and chemical vapor deposition [10]. However, these techniques are limited due to their complicated processes, high cost and poor mechanical properties of the surface structures.

Recently, laser surface texturing is regarded as one of the simple and effective approaches to directly acquire super-hydrophobic surfaces on a wide variety of material surfaces. It can provide a precise control to fabricate stable 3D hierarchical structures which are essential to prolong surface durability [11]. However, many previous studies have reported that just after laser ablation, the fresh ablated metal surface was hydrophilic or super-hydrophilic with the presence of micro/nanostructures. When the laser ablated surface was exposed to the ambient air for a relatively long time, the wettability transition from super-hydrophilic to super-hydrophobic could be observed [12-20]. Recent research efforts have been directed towards the explanation of the wettability transition mechanism. For example, Kietzig et al. [21] suggested the decomposition of CO_2 into carbon with active magnetite created in the laser irradiation process as the potential reason for the wettability transition from hydrophilicity to hydrophobicity. Long et al. [22] experimentally verified that a rich CO_2 condition could restrain the wettability transition to super-hydrophobic state. Ta et al. [23] reported that the wettability change of laser ablated copper surface was due to the partial deoxidation of outer layer of hydrophilic CuO into hydrophobic Cu_2O. However, Boinovich et al. [24] commented Ta's work and revealed that the actual reason for super-hydrophobicity was adsorption of airborne hydrocarbon contaminations on laser ablated copper surface.

Obviously, no reasonable mechanism is well-accepted to explain the wettability change of laser ablated surfaces under ambient air exposure. Moreover, in terms of immediate super-hydrophilicity on the fresh laser ablated surfaces, previous research only proposed one factor that laser-induced micro/nanostructures should account for the super-hydrophilicity according to Wenzel theory, while only a few studies explained this phenomenon in respect of surface chemistry analysis. Even though Long et al. [25] mentioned this aspect and proposed this super-hydrophilicity was related with the outer layer of hydrophilic oxide, they did not explain how the oxide layer was formed and why the laser-induced oxide layer was super-hydrophilic. It is therefore required to systematically investigate the whole mechanism of wettability transition on the laser ablated surfaces.

In this paper, the wettability transition mechanism was systematically investigated by analyzing surface morphology and surface chemical compositions of the following four samples: the bare aluminum surface (Al-I), fresh laser ablated super-hydrophilic surface (Al-II), 15-day air exposed hydrophobic surface (Al-III) and aged super-hydrophobic surface (Al-IV). It is noted that the Al-II surface was super-hydrophilic and then gradually reached super-hydrophobic when exposed to ambient air for 30 days. It can be concluded that based on the Wenzel [26] and Cassie-Baxter theory [27], the laser-induced rough hierarchical structures had an amplification effect on both fresh super-hydrophilicity and aged super-hydrophobicity. In terms of surface chemistry analysis, the immediate super-hydrophilicity was attributed to the decrease of surface nonpolarity (relative carbon content and hydrocarbon concentration) and the increase of surface polarity (formation of hydrophilic alumina and residual unsaturated atoms). The super-hydrophobicity of Al-IV surface was related with the organic matters absorbed from air moisture. The mechanism of wettability transition was extensively discussed in Section 3.4. The thermal annealing experiment was performed to further validate the established theory and analyses. Surface stability is very significant for the practical applications of the super-hydrophobic surfaces. Therefore, in this study, the surface stability of laser ablated super-hydrophobic surfaces that were stored in ambient air was also discussed.

2. Experimental

2.1. Material

The experiment was performed on 1060 aluminum substrates (high-purity 99.6%) with the size of 20 mm × 20 mm × 1 mm. The acetone and ethanol (AR, >99%) were purchased from Beijing Chemical Works. The distilled water was provided by a UCP-III water purification system. All chemicals were used as received without further purification. Before laser ablation, the samples were mechanically polished to obtain surface roughness under 1 μm, then ultrasonically washed with acetone, ethanol and deionized water in sequence to remove surface contaminants. The rinsed samples were dried by compressed nitrogen.

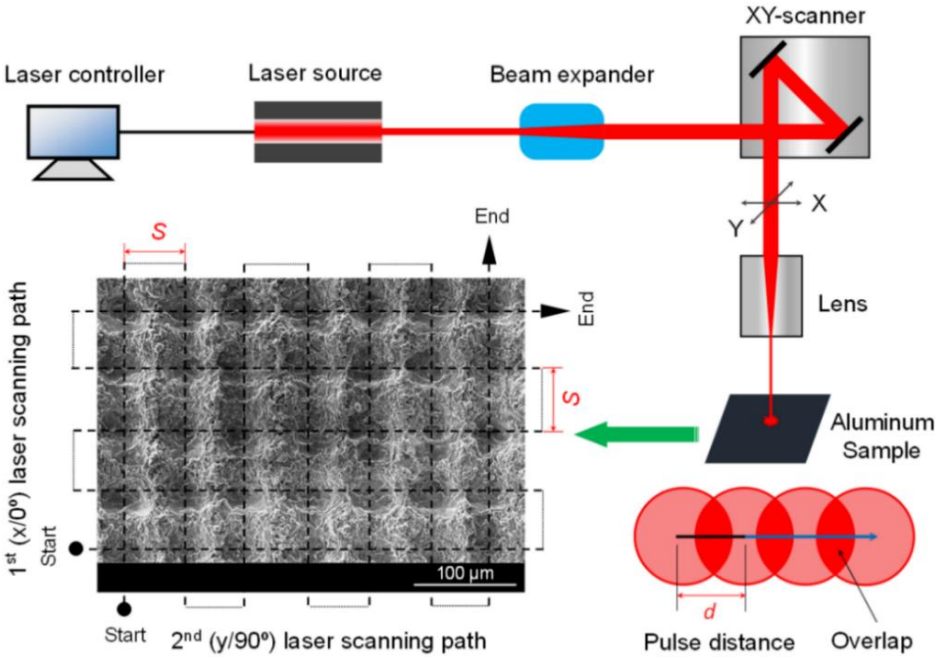

Figure 1. The demonstration of laser system and pulse overlap; schematic explanation of laser scanning path and SEM image of the laser ablated surfaces.

2.2.Laser processing

Table 1. Laser processing parameters

Average laser power, P (W)	10
Repetition rate, f (kHz)	20
Spot diameter, D (μm)	50
Laser fluence, F (J/cm^2)	25.46
Spacing, S (μm)	60
Scanning speed, V (mm/s)	500

The polished samples were ablated by a nanosecond Ytterbium fiber laser source (IPG photonics from Germany) with a wavelength of 1064 nm, output power of 10 W, pulse duration of 50 ns and repetition rate up to 20 kHz. A scanning head with a focusing lens was applied for the delivery of focused laser beam. Fig. 1 demonstrates the components of laser processing system. The samples fixed on the working platform were ablated by the moving laser beams, first along the x (0°) and then along the y (90°) directions (dashed lines in Fig. 1). The spacing (S) between adjacent laser scanning lines was 60 μm in the two perpendicular directions, which resulted in micro-grooves on the laser ablated surface. The experiments were performed using the ablation parameters as shown in Table 1.

2.3.Measurement and characterization

The effect of laser ablation on surface morphology was studied by means of SEM (FEI, Quanta 250 FEG). 3D image and cross-sectional profile were obtained using stylus profilers (Bruker, Dektak). The wetting property was examined by static contact angle using a goniometer (AST, VCA optima). A droplet with volume of 8 μL distilled water was dispensed on laser ablated samples. Here, the contact angles were recorded everyday by measuring different samples, treated by the same laser parameters but exposed to ambient air (temperature = 25°C, humidity = 50%) for different periods. In order to explore the wettability transition mechanism, surface chemical compositions of the bare Al-I, fresh Al-II, 15-day exposed Al-III and aged Al-IV and annealed surfaces were evaluated by XPS (Thermo Fisher Scientific, Escalab 250Xi). The XPS data was analyzed in CasaXPS software.

3. Results and discussion

3.1. Analysis of surface microstructures

Surface morphology was significantly changed after laser ablation. Based on the laser parameters displayed in Table 1, the number of laser pulses per spot and overlapping factor (*OF*) could be calculated. As illustrated in Fig. 1, pulse distance $d = V/f$ with V as the scanning speed and f the repetition rate, so the pulses number per spot was 2. The accumulated overlapped factor (*OF*) of 39.09% can be obtained by Eq. (1) [28]:

$$OF = \frac{2}{\pi D}\left\{ D\arccos\left(\frac{d}{D}\right) - d\sqrt{1-\left(\frac{d}{D}\right)^2} \right\} \quad (1)$$

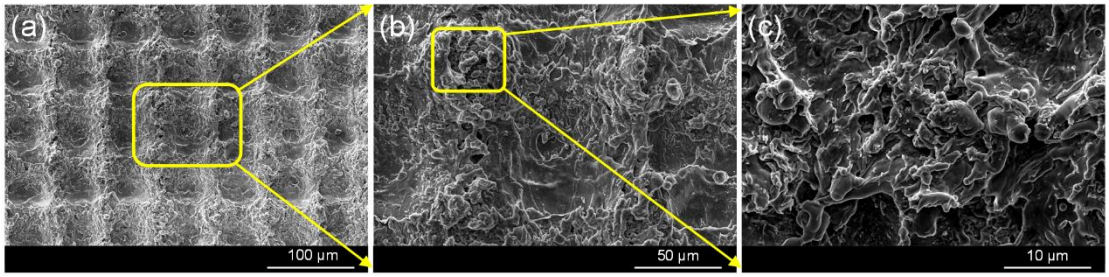

Figure 2. SEM images of laser ablated aluminum surface: (a) large-area view, (b) further magnified image, (c) higher magnification image of the protrusion.

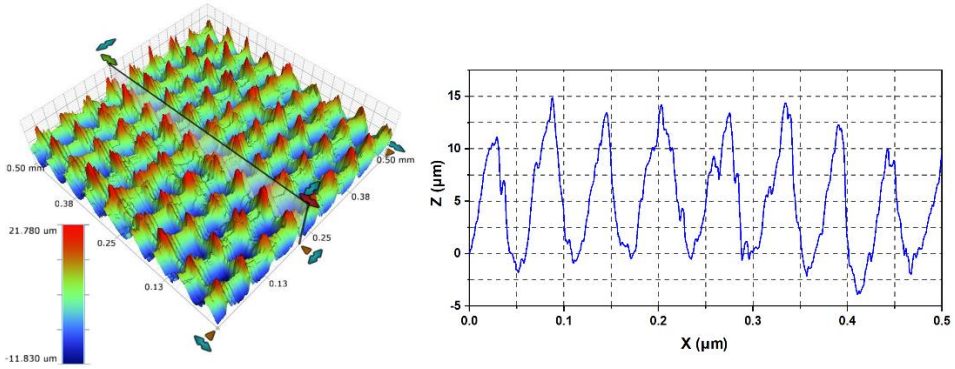

Figure 3. 3D and cross-sectional profiles of the laser ablated aluminum surface.

Figs. 2a-c show the typical SEM images of the laser ablated aluminum surface, where the surface was ablated to form a micro/nanoscale rough structure with large numbers of protrusions and covered particles. As shown in Fig. 3, the average width and depth of the laser induced µ-grooves were 55.96 µm and 15.16 µm, respectively. The enlarged SEM image shows the inside wall and the brim of µ-grooves were randomly deposited with many irregular particles (Fig. 2b). The line-by-line laser scanning with spacing of 60 µm was applied along the two perpendicular directions, which resulted in the formation of periodic protrusions since the spacing value was almost the same with the width of laser ablated grooves. It can be seen from Fig. 2c that many irregular particles with size of nanometers to micrometers were decorated on each protrusion, therefore the hierarchical rough structure was formed after nanosecond laser ablation. The generation of micro/nano-scaled dual structure could be attributed to laser irradiation that caused an increase temperature on the aluminum surface due to the absorbed laser energy. When the center of the pulsed area was melted and vaporized,

the groove was created, and numerous randomized micro/nanoparticles on the protrusions were formed because of the accumulation of ejected materials. Thus, the μ-grooves combined with particles and periodic protrusions generated the hierarchical surface structures, whereby large air pockets were trapped, reducing the contact area between the actual surface and the liquid droplet.

3.2.Wettability evolution

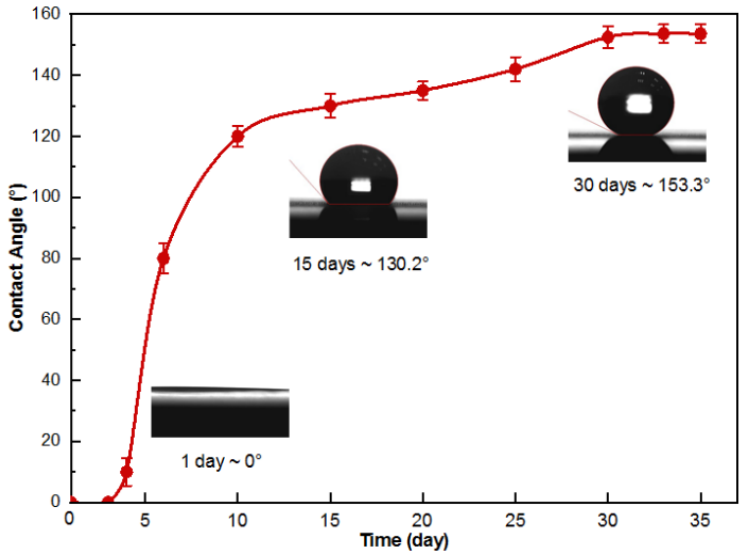

Figure 4. Time-dependence of WCAs for the laser ablated surfaces stored in ambient air.

Table 2. RAs evolution of the as-prepared surface over time.

Sample No.	RA	Image
Bare surface (Al-I)	No	
1-day air exposure (Al-II)	No	
5-day air exposure	No	
15-day exposure (Al-III)	No	
20-day exposure	No	
25-day exposure	80.5 ± 9.0º	
30-day exposure (Al-IV)	5.5 ± 1.5º	
35-day exposure	5.0 ± 2.0º	

Surface wettability of the laser ablated samples was evaluated via measuring their static WCAs and RAs. Each measured value was averaged over three locations. The growth of WCA indicates a decline in wetting property. Fig. 4 depicts the time-dependence of WCAs for the as-prepared surfaces when they were exposed to ambient air, and the evolution of their corresponding RAs as a function of time is summarized in Table 2. Before laser treatment, the bare Al-I surface was hydrophilic due to its WCA only 85.0 ± 3.0º. Once ablated by laser, the fresh Al-II surface immediately exhibited a super-hydrophilic behavior, and the water droplet can fully spread out when it touched the laser-induced rough surface. It was unable to acquire WCA value as the droplet was almost completely penetrated into the grooves (see the bottom-left image inserted in Fig. 4). This phenomenon was well pronounced within 3 days after laser ablation. The occurrence of super-hydrophilicity was possibly related with surface morphology modification. According to Wenzel theory, the increase of surface roughness leads to an amplification effect on surface wettability [26].

$$\cos\theta_w = r\cos\theta_f \tag{2}$$

Where r >1 is surface roughness parameter, θ_f and θ_w represent WCAs for the flat and rough surfaces, respectively. Eq. (2) reveals that with the enhancement of surface roughness, a hydrophilic surface will become more hydrophilic and a hydrophobic surface will become more hydrophobic. Therefore, at early stage of WCA evolution, the fresh Al-II surface exhibited a very small contact angle due to the increment of roughness. Another possible reason for the observed super-hydrophilicity might be the change of surface chemical compositions before/after laser ablation. This aspect is usually ignored in previous studies and will be elaborately introduced in the next section.

Observing contact angle curve in Fig. 4, it is noted that when the laser ablated surface was exposed to air, its surface hydrophilicity decreased due to the increase of WCA over time. Between Day 4 and Day 15, the WCA witnessed a sharp increase from 10.5º to 130.2º. It is noted that fresh Al-III surface reached hydrophobic behavior. However, although the WCA value was significantly increased and the contact area between the sample surface and water droplet was reduced, there was still no RA

because the water droplet was still firmly stuck onto the laser ablated surfaces, even if the samples were positioned vertically (as shown in Table 2) [29]. With the extension of air exposure time, the WCA of 143.2 ± 2.5º and RA of 80.5 ± 9.0º were obtained when the as-prepared surface was exposed to ambient air for 25 days. Over a period of 30 days, the WCA gradually increased to a relatively stable state with WCA of 153.3 ± 2.5º and RA of 5.5 ± 1.5º, which can be characterized as a typical super-hydrophobic surface. Thus, we can conclude that after laser ablation, the fresh laser-induced surface showed super-hydrophilic property, then gradually turned to super-hydrophobic state when exposed to ambient air for one month.

3.3.Analysis of surface chemistry

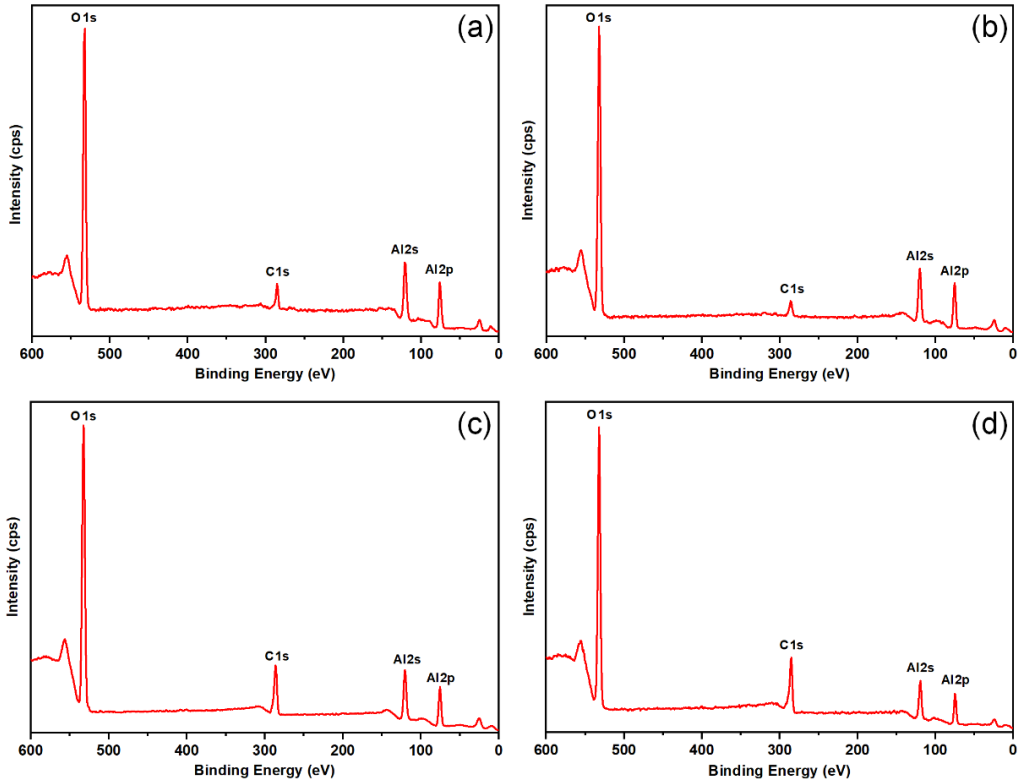

Figure 5. XPS spectra of (a) bare Al-I surface, (b) fresh Al-II surface, (c) 15-day air exposed Al-III surface and (d) aged Al-IV surface.

In order to probe the time-dependence of surface wettability before and after laser treatment, surface chemistry was examined by XPS. Fig. 5 displays the XPS spectra of the bare Al-I surface, fresh Al-II surface, 15-day air exposed Al-III surface and aged Al-IV surface, and their corresponding surface chemical composition analyses are presented in Table 3. By observing the exhibited results one can confirm that three main

elements C, O and Al constitute these surfaces, and the C 1s peak, O 1s peak and Al 2p peak were around 285.0, 532.2 and 75.5 eV, respectively. The influences of other elements were not considered due to very low content. We therefore only plot the binding energy from 0 to 600 V in the XPS spectra so as to clearly show the variation of carbon content. By analyzing the peaks of binding energies, it can be deduced that aluminum was mainly present in the form of alumina, and the detected carbon was related with the adsorption of hydrocarbon organic matters from ambient air.

Table 3. Chemical compositions measured by XPS.

Sample	Al (at.%)	C (at.%)	O (at.%)	C/Al	O/Al
Al-I	35.45	13.17	51.38	0.37	1.45
Al-II	33.74	9.04	57.22	0.26	1.69
Al-III	25.01	25.60	49.39	1.02	1.97
Al-IV	23.43	30.03	46.54	1.28	1.98

It is common that as an active metal, rapid passivation will occur on the pure aluminum surface. Therefore, the bare non-treated Al-I surface was covered with a thin film of aluminum oxide, which could be confirmed by the Al $2p_{3/2}$ peak at 75.6 eV and O 1s peak at 532.2 eV and by the approximate O/Al ratio of 1.45 for the Al_2O_3 stoichiometry. If the aluminum oxide surface was clean and free of pollution, the carbon content should be zero. But XPS results indicated that over 13% carbon was detected on bare Al-I surface. This additional carbon may derive from two main sources: the residual oil in the vacuum chamber of XPS equipment and adsorption of airborne contaminants (organic matters) in the period from sample cleaning procedure to XPS measurement. In this study, the relative amount of attached organic matters could be characterized by the C/Al ratio, represented the atomic carbon content relative to the atomic aluminum content.

It has been reported that such adsorbed organic matters on aluminum oxide would result in more detected carbon and less aluminum because of short depth of XPS analysis (approximately 7 nm for C 1s photoelectrons and 8 nm for Al 2p photoelectrons) [28]. However, immediately after laser ablation, the carbon content and C/Al ratio showed a noticeable decline on the fresh super-hydrophilic Al-II surface, which could

be ascribed to the destruction of initial absorbed organic molecules by the laser beam incidence. Meanwhile, as shown in Table 3, the oxygen content and O/Al ratio increased on the Al-II surface, indicating that the aluminum surface was oxidized because of the effect of laser ablation. Once the grooves were created during the laser processing, more internal pure aluminum was exposed to the ambient air and the fast passivation resulted in the generation of an outer layer of alumina (Al_2O_3). Therefore, oxidation effect could be another dominated cause for wettability change from bare hydrophobicity to fresh super-hydrophilicity, apart from the modification of surface morphology by laser ablation,

When the laser ablated surface was exposed to ambient air beyond 15 days, the Al-III surface showed a significant increase in carbon content as well as C/Al ratio on the formed hierarchical rough structures. It can be deduced that the main reason for time-dependence of WCAs might be related with the change of surface chemical compositions since there was no change for the surface morphology during the ageing process under the ambient air. We conjecture that the obvious increase of carbon content was probably due to the adsorption of organic matters from the ambient air. It can be further verified that after the laser ablated surface was stored in ambient air for 30 days, as shown in Fig. 5 and Table 3, XPS results imply that the carbon content and the C/Al ratio on aged super-hydrophobic Al-IV surface sustainably increased to 30.03% and 1.28, respectively. Interestingly, it is noted that the trends of carbon content and C/Al ratio among these surfaces coincided well with their corresponding WCAs: the surface with high WCA always had a relatively large C/Al value. The authors believe that the increase of carbon during the ageing process resulted from the absorption of airborne hydrocarbon contaminants onto the surface of aluminum oxide.

In order to further investigate surface polarity of the four surfaces and verify the proposed assumption, the high resolution of C 1s spectra were carried out in the CasaXPS software. The C 1s peak was decomposed into four components. The component of hydrocarbon chains or graphitic structure (C-C(H)) took up the peak position around 284.7 eV. Other three functional groups of C-O, C=O and O-C=O were also resolved, which might come from the absorption of alcohols/ether,

aldehydes/ketones and carboxyl/ester matters, respectively. The peak positions of C-O, C=O and O-C=O component were fixed at around 285.6, 287.5 and 289.6 eV, respectively. In general, the functional group of C-C(H) is regarded as nonpolar and contributes to the hydrophobic property, while other three functional groups of ether, carbonyl and carboxyl are hydrophilic due to high polarity [22]. Thus, the relative concentration of C-C(H) bond can be an indicator to characterize surface wetting property.

Figs. 6 depicts the component of surface functional groups for the bare Al-I sample, fresh Al-II sample, 15-day air exposed Al-III sample and aged Al-IV sample. It is noted that the surface chemical compositions of the samples stored in ambient air for different period changed a great deal from their initial state. To clearly display these changes, the comparison of relative concentration of C-C(H) group on various surfaces was summarized in Fig. 7. The results confirm that compared with the bare Al-I surface, the fresh Al-II surface experienced a dramatic decrease of C-C(H) concentration from 45.73% to 31.31%, resulting in the super-hydrophilic state because of the dominance of polar sites. For the sample exposed to the ambient air for 15 days, the C-C(H) concentration on the Al-III surface showed a considerable increase to 56.25%, indicating that the Al-III surface was dominated by nonpolar groups with lower surface free energy and therefore exhibited hydrophobic property.

When the exposure time prolonged to 30 days, the Al-IV surface exhibited super-hydrophobic state, and the highest concentration of nonpolar C-C(H) group at 62.04% could account for its super-hydrophobicity. The accumulation of carbon content and nonpolar group indicated that some organic matters in air moisture were absorbed on the laser ablated surface during the ageing process. Various organic matters in air moisture have short chain organic molecules that are nonpolar, such as formic and acetic acid [30]. Due to the carboxylation effect, these nonpolar chains will be chemisorbed onto the laser ablated surface and gradually lower the surface free energy. Thus, the wettability transition during the ageing process was attributed to the depolarization effect, which will be discussed in detail later.

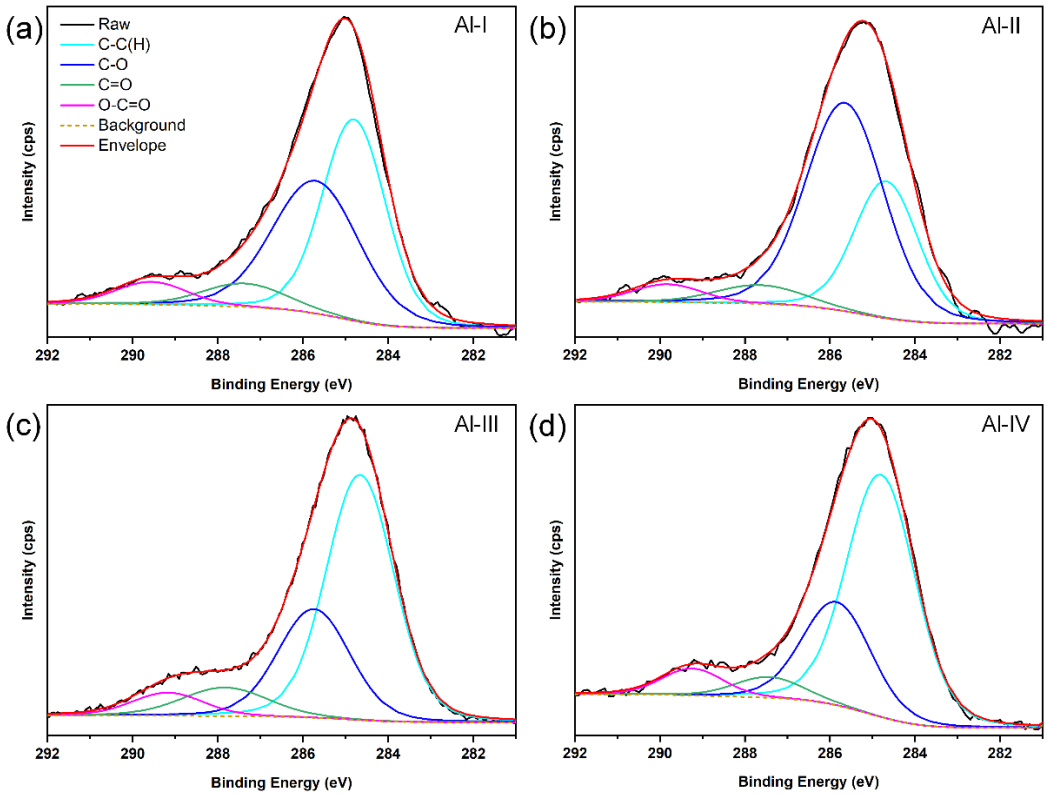

Figure 6. High resolution of C 1s spectra of different surfaces: (a) Al-I surface, (b) Al-II surface, (c) Al-III surface, (d) Al-IV surface.

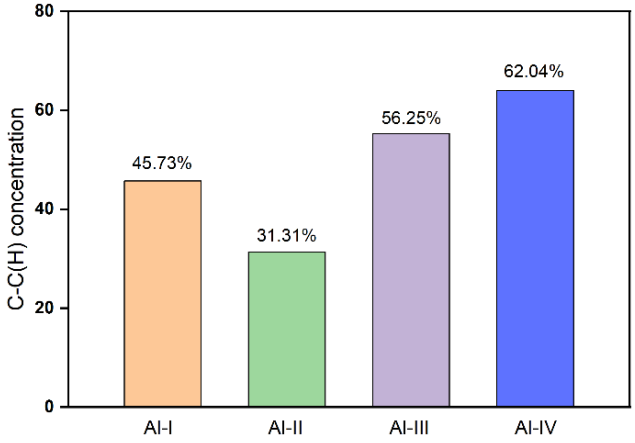

Figure 7. Comparison of relative concentration of C-C(H) group (at.%) on various surfaces.

3.4. Mechanism of wettability transition

Surface polarity (i.e., total surface free energy) definitely determines surface wetting property: the increased surface polarity generally results in higher hydrophilicity [31]. Laser ablation resulted in the formation of grooves, and more internal pure aluminum atoms were exposed to the ambient air then quickly became alumina due to the rapid passivation. Additionally, laser irradiation could generate many atoms in the form of Al^{3+} and O^{2-} that gradually organized on a lattice to create

alumina [28]. This alumina was hydrophilic because it had large numbers of polar sites originating from unsaturated aluminum and oxygen atoms that acted as strong Lewis acid and base pairs, respectively [32]. The state of molecules/atoms on the fresh Al-II surface can be displayed in Fig. 8. These aluminum atoms were electron-deficient with only six electrons in their sp^2-hybrid orbitals. Therefore, these atoms should generate a hydrogen bond with water molecules to gain a full octet of electrons, resulting in the hydrophilic hydration structure [33]. It is also reported that a considerable number of unsaturated Al^{3+} and O^{2-} were not immediately paired, leading to dramatical growth of surface polarity [32]. Hence, immediately posterior to laser processing, it can be concluded that the fresh laser ablated surface was highly non-equilibrium, contained many surface defects and thus presented very high surface polarity, which caused the super-hydrophilic behavior. Combined with the above discussion of carbon content, the super-hydrophilicity of the fresh Al-II surface was physically and chemically analyzed in this study. The results confirm that the immediate super-hydrophilicity was ascribed to the decrease of surface nonpolarity (characterized by C/Al value and relative C-C(H) concentration) and increase of surface polarity (analyzed from the prospects of the formation of hydrophilic alumina and residual unsaturated atoms).

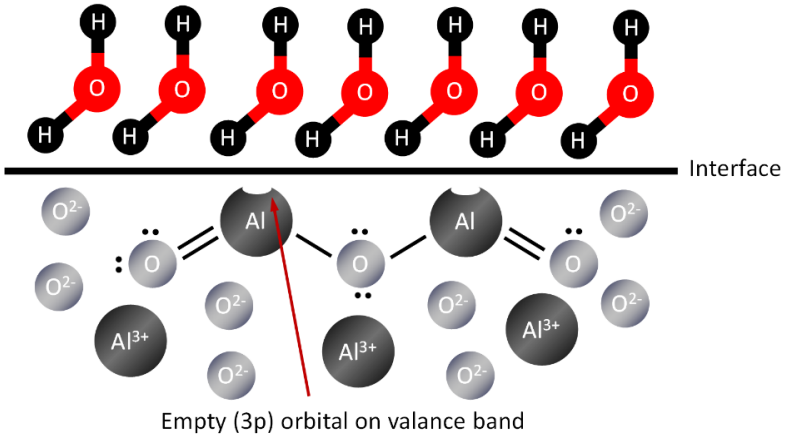

Figure 8. Schematic illustration of molecules/atoms state of the fresh Al-II surface.

When the laser ablated surface was exposed to ambient air, the wettability transition from super-hydrophilic to super-hydrophobic was related with the absorbed organic compounds [11, 22, 34]. During the transition process, surface hydroxylation plays an important role. This is because Lewis acid and base pairs were rapidly

hydroxylated when they reacted with OH^- and H^+ dissociated from interfacial water vapor molecules, resulting in a weakness of Lewis acid-base sites and reducing the total surface free energy of alumina. But surface hydroxylation cannot explain the gradual change of WCAs since hydroxylation process is very fast. Additionally, the hydroxides show very high adhesion to water molecules, and thus hydroxylation should not be the direct reason for super-hydrophobicity. However, the organic matters such as carboxylates can be chemisorbed onto the laser ablated surfaces by the interaction with hydroxyls formed in the hydroxylation process. The schematic illustration of chemisorption mechanism is clearly presented in Fig. 9, and the corresponding chemical reaction can be explained by the following Eq. (3).

$$\text{Al-OH} + \text{RCOOH}_{(g)} \rightarrow \text{RCOO-Al} + \text{H}_2\text{O} \quad (3)$$

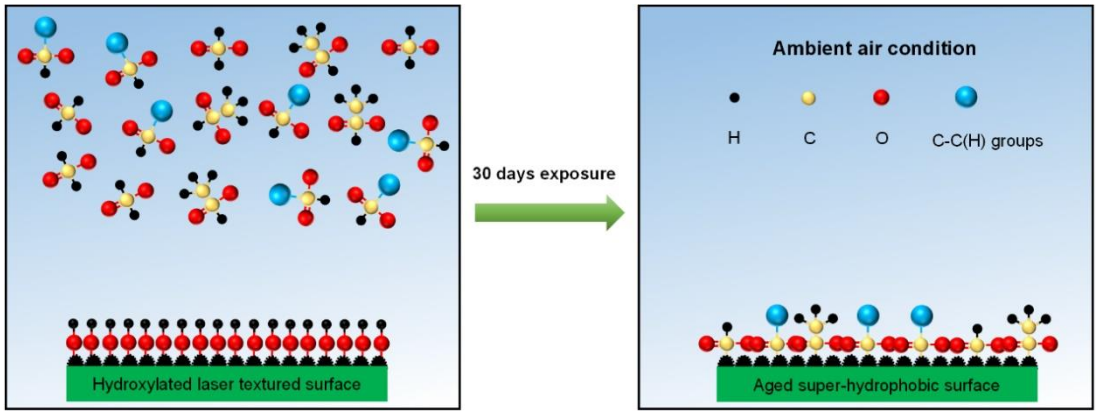

Figure 9. Schematic illustration of chemisorption mechanism in ageing process.

Once the carboxylates in air moisture such as formic and acetic acid were absorbed, their nonpolar chain *R* containing C-C(H) groups were attached onto the outer layer of the surface, lowering the total surface free energy [30]. This depolarization process is slow and therefore can account for the gradual transition from super-hydrophilicity to super-hydrophobicity. To further verify this assumption, the concentration of O-C=O group is also examined by decomposing O 1s spectra of the fresh Al-II surface and the aged Al-IV surface. The O 1s spectra displayed in Fig. 10 is resolved into four peaks over the binding energies of 531.2, 532.2, 532.8 and 533.8 eV, corresponding to the Al_2O_3, C=O/C-O, Al-OH and O-C=O, respectively [35]. The results infer that the oxygen on fresh Al-II surface came primarily from alumina (Al_2O_3) due to the oxidation effect by laser, while the relative concentration of O-C=O group was only 7.60%. After

the laser ablated surface was exposed to ambient air for one month, the O-C=O concentration significantly increased to 21.77% on the aged Al-IV surface. Thus, combined with the increase of C-C(H) concentration on the aged super-hydrophobic surface, it can further confirm that the carboxylates containing nonpolar molecules were chemisorbed on the laser ablated surface, resulting in the gradual decrease of surface free energy.

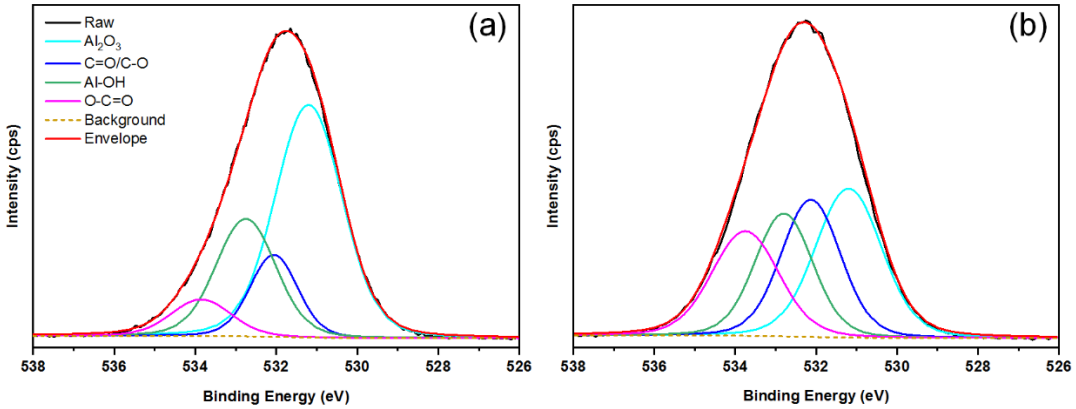

Figure 10. High resolution of O 1s spectra: (a) fresh super-hydrophilic Al-II surface, (b) aged super-hydrophobic Al-IV surface.

Apart from surface polarity, the rough hierarchical structures induced by laser ablation is another reason for the wettability changes. As discussed above, just after laser ablation, the fresh Al-II surface was modified with a rough layer of hydrophilic alumina. When a water droplet was dispensed on this rough surface, the liquid quickly penetrated into the grooves. Finally, the water droplet was completely spread on the fresh Al-II surface which could be modeled by Wenzel state in this case. The Wenzel state reveals that the contact angle will decrease with the increasing of surface roughness for an intrinsic hydrophilic surface, whereas the contact angle will become larger when the surface roughness of a hydrophobic surface increases. Therefore, the created rough hierarchical structures on hydrophilic aluminum surface amplified the effect of hydrophilicity, resulting in a super-hydrophilic property just after laser ablation. After being exposed to ambient air for almost one month, the laser ablated surface became super-hydrophobic due to the chemisorbed nonpolar organic chains from air moisture. The dispensed water droplet could not fill the grooves due to the generation of a solid-air composite interface, and thus this surface can be modeled by Cassie-

Baxter state. In this case the rough structures had an amplification influence on hydrophobicity and therefore the aged surface gradually turned to super-hydrophobic.

3.5. Thermal annealing experiment

Many studies have reported that thermal annealing can partially remove the adsorbed organic contaminants [36-37]. In order to further verify the effect of adsorbed organic matters on surface wettability, the aged super-hydrophobic Al-IV surface was annealed in Ar at 350 °C for 2h. We found that no obvious change of surface morphology was observed on the annealed sample, but its WCA suddenly decreased to 11.9 ± 3.5º with no existing of RA value. When it is exposed to ambient air again, the annealed surface exhibited a rapid growth of WCA, with similar behavior for the as-prepared surface. XPS results imply that the relative carbon content (C/Al) on the annealed surface was dramatically decreased to 0.96 compared to 1.28 on the aged super-hydrophobic surface (as displayed in Fig. 11a), indicating that the absorbed organic compounds were partially removed after annealing process. Furthermore, it is noted from Fig. 11b that the annealed surface was dominated by the polar functional groups because the C-C(H) concentration was reduced to 39.78%. Therefore, the thermal annealing experiment could verify that the gradual increase of WCA was attributed to the absorbed organic matters from air moisture. Additionally, annealing experiment demonstrated that the relative carbon content value (C/Al) and C-C(H) concentration could be the indicator for surface polarity: the higher C/Al value and C-C(H) concentration would lead to more hydrophobic surface.

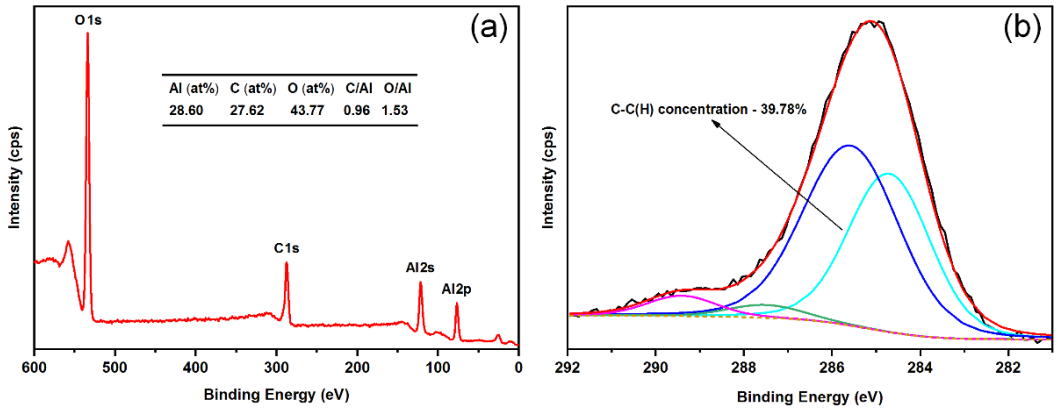

Figure 11. (a) XPS spectrum of the annealed surface, (b) High resolution of C 1s spectra and relative concentration of C-C(H) group.

3.6. Surface stability

Surface stability is an important factor to determine whether the fabricated super-hydrophobic surfaces are suitable for industrial multifunctional applications. Therefore, the stability of the as-prepared super-hydrophobic is also discussed in this work. The results demonstrate that the laser ablated aluminum surface will require around one month to reach super-hydrophobic state, exhibiting a WCA of 153.3 ± 2.5º and RA of 5.5 ± 1.5º. Then if this typical super-hydrophobic surface was continually exposed to the ambient air for four months, the surface could maintain its super-hydrophobic property. It can be noted that the laser ablated surface still presented a high WCA of 152.8° ± 2.5º with a small RA of 6.5 ± 2.0º (as shown in Fig. 12), which indicates that the laser ablated super-hydrophobic surfaces showed excellent surface stability regarding distilled water (PH = 7) when they were stored in the ambient air. However, the thermal annealing experiment proved that this laser-induced super-hydrophobic would turn to hydrophilic, implying that the thermal stability of this kind of super-hydrophobic surface was relatively weak because it cannot bear high temperature.

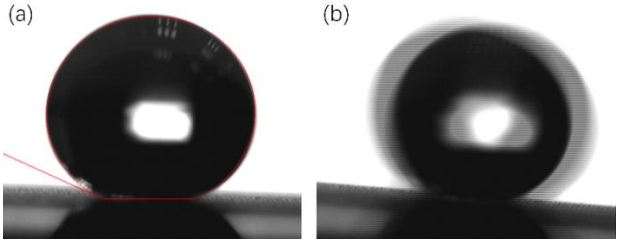

Figure 12. (a) WCA and (b) RA measurement on the as-prepared surface that was exposure to ambient air for four months.

This present study mainly focused on the investigation of wettability transition mechanism, and it conclusion is that the gradual wettability transition from super-hydrophilic to super-hydrophobic was attributed to the spontaneous adsorption of organic matters onto the laser ablated rough surfaces. However, the physically adsorbed organic matters will hardly be well ordered, and this kind of super-hydrophobic surface may be very sensitive to other liquid media, such as the aqueous media with different PH or salinity [24]. Therefore, such super-hydrophobic layer can easily be removed because of the interaction liquid media, causing the instability and uncontrolled loss of super-hydrophobicity. This will lead to failure of such surfaces in industry, specifically

the outdoor applications. Future investigations on the thermal stability, mechanical stability and chemical stability of the laser ablated super-hydrophobic surfaces will be performed.

4. Conclusions

In this study, a rough surface with micro/nanostructures was simply formed on the aluminum substrate by one-step nanosecond laser ablation. We found that the fresh laser ablated surface was super-hydrophilic, and then gradually reached super-hydrophobic state after exposed to ambient air for one month. The time-dependent wettability (i.e., the wettability transition mechanism) of the laser ablated surface was systematically investigated by analyzing the changes of surface morphology and surface chemical compositions before/after laser ablation. The results clearly indicated that the laser-induced hierarchical structures had the amplified effects on the fresh super-hydrophilicity and aged hydrophobicity according to the Wenzel and Cassie-Baxter theory, respectively. The analyses of the surface chemistry revealed that the immediate super-hydrophilic transition was attributed to the decrease of nonpolar carbon and the formation of hydrophilic alumina as well as the residual unsaturated atoms. Besides, the gradual super-hydrophilic to super-hydrophobic transition was related with the chemisorbed organic matters from the air moisture, which can be validated by the thermal annealing experiment. Compared to previous literature, we particularly described how the alumina was formed just after laser ablation and why the fresh laser ablated surface was super-hydrophilic in terms of the changes of surface chemical compositions. Moreover, the chemisorption mechanism of the organic matters onto the laser-induced surfaces was also proposed. Surface stability is an important factor for the super-hydrophobic to be used in industrial applications. Therefore, the future work on thermal stability, mechanical stability and chemical stability of such laser ablated super-hydrophobic surfaces will be performed. It is believed that this study can help researchers understand the formation mechanism of laser-induced super-hydrophobic surfaces and can further guide industry to modify surface chemistry to effectively produce durable and stable super-hydrophobic coatings.

Acknowledgements

We gratefully acknowledge financial supports from H2020-MSCA-RISE Project (FabSurfWAR-644971), China-EU H2020 International Science and Technology Cooperation Project (2016YFE0112100) and National Natural Science Foundations of China (Nos. 51675371, 51675376 and 51675367). The authors also acknowledge Prof. Zuobin Wang in Changchun University of Science and Technology (CUST) for technique supports.

References:

[1] J.A. Maurer, M.J. Miller, S.F. Bartolucci, Self-cleaning superhydrophobic nanocomposite surfaces generated by laser pulse heating, J. Colloid. Interface. Sci. 524 (2018) 204-208.

[2] G.D. Bixler, B. Bhushan, Shark skin inspired low-drag microstructured surfaces in closed channel flow, J. Colloid. Interface. Sci. 393 (2013) 384-396.

[3] Y.B. Zhao, L.Q. Shi, X.J. Ji, J.C. Li, Z.Z. Han, S.L. Li, R.C. Zeng, F. Zhang, A.L. Wang, Corrosion resistance and antibacterial properties of polysiloxane modified layer-by-layer assembled self-healing coating on magnesium alloy, J. Colloid. Interface. Sci. 526 (2018) 43-50.

[4] M.C. Lu, C.C. Lin, C.W. Lo, C.W. Huang, C.C. Wang, Superhydrophobic Si nanowires for enhanced condensation heat transfer, Int. J. Heat Mass Tran. 111(2017) 614-623.

[5] C.V. Ngo, D.M. Chun, Control of laser-ablated aluminum surface wettability to superhydrophobic or superhydrophilic through simple heat treatment or water boiling post-processing, Appl. Surf. Sci. 435(2018) 974-982.

[6] S.F. Toosi, S. Moradi, M. Ebrahimi, S.G. Hatzikiriakos, Microfabrication of polymeric surfaces with extreme wettability using hot embossing, Appl. Surf. Sci. 378 (2016) 426-434.

[7] R.V. Lakshmi, B.J. Basu, Fabrication of superhydrophobic sol-gel composite films using hydrophobically modified colloidal zinc hydroxide, J. Colloid. Interface. Sci. 339 (2009) 454-460.

[8] J. Cremaldi, B. Bhushan, Fabrication of bioinspired, self-cleaning superliquiphilic/phobic stainless steel using different pathways, J. Colloid. Interface. Sci. 518 (2018) 284-297.

[9] Y. Liu, S.Y. Li, Y.M. Wang, H.Y. Wang, K. Gao, Z.W. Han, L.Q. Ren, Superhydrophobic and superoleophobic surface by electrodeposition on magnesium alloy substrate: Wettability and corrosion inhibition, J. Colloid. Interface. Sci. 478 (2016) 164-171.

[10] S.A. Kamal, R. Ritikos, S.A. Rahman, Wetting behavior of carbon nitride nanostructures grown by plasma enhanced chemical vapor deposition technique, Appl. Surf. Sci. 328 (2015) 146-153.

[11] H.P. Yan, M.R. Rashid, S.Y. Khew, F.P. Li, M.H. Hong, Wettability transition of laser textured brass surfaces inside different mediums, Appl. Surf. Sci. 427 (2018) 369-375.

[12] Z. Yang, Y.L. Tian, C.J. Yang, F.J. Wang, X.P. Liu, Modification of wetting property of Inconel 718 surface by nanosecond laser texturing, Appl. Surf. Sci. 414 (2017) 313-324.

[13] D.M. Chun, C.V. Ngo, K.M. Lee, Fast fabrication of superhydrophobic metallic surface using nanosecond laser texturing and low-temperature annealing, CIRP Ann-Manuf. Techn. 65 (2016) 519-522.

[14] M.M. Calderon, A. Rodriguez, A.D. Ponte, M.C. Morant-Minana, M.G. Aranzadi, S.M. Olaizola. Femtosecond laser fabrication of highly hydrophobic stainless steel surface with hierarchical structures fabricated by combining ordered microstructures and LIPSS, Appl. Surf. Sci. 374 (2016) 81-89.

[15] L.B. Boinovich, A.M. Emelyanenko, A.D. Modestov, A.G. Domantovsky, K.A. Emelyanenko, Synergistic effect of superhydrophobicity and oxidized layers on corrosion resistance of aluminum alloy surface textured by nanosecond laser treatment, ACS Appl. Mater. Interfaces 7 (2015) 19500-19508.

[16] C.J. Yang, X.S. Mei, Y.L. Tian, D.W. Zhang, Y. Li, X.P. Liu, Modification of wettability property of titanium by laser texturing, Int. J. Adv. Manuf. Technol. 87 (2016) 1663-1670.

[17] R. Jagdheesh, J.J. García-Ballesteros, J.L. Ocaña, One-step fabrication of near superhydrophobic aluminum surface by nanosecond laser ablation, Appl. Surf. Sci. 374 (2016) 2-11.

[18] B.S. Yibas, H. Ali, M. Khaled, N.A. Aqeeli, N.A. Dheir, K.K. Varanasi. Characteristics of laser textured silicon surface and effect of mud adhesion on hydrophobicity, Appl. Surf. Sci. 351 (2015) 880-888.

[19] N. Mirhosseini, P.L. Crouse, M.J.J. Schmidth, L. Li, D. Garrod. Laser surface micro-texturing of Ti6Al4V substrates for improved cell integration, Appl. Surf Sci. 253 (2007) 7738-7743.

[20] Z.S. Guan, Q. Zhang. Effect of topography on wettability of pulse laser-ablated Si surface, Acta Chimica Sinica. 63 (2005) 880-884.

[21] A.M. Kietzig, S.G. Hatzikiriakos, P. Englezos, Patterned superhydrophobic metallic surfaces, Langmuir 25 (2009) 4821-4827.

[22] J. Long, M. Zhong, H. Zhang, P. Fan, Superhydrophilicity to superhydrophobicity transition of picosecond laser microstructured aluminum in ambient air, J. Colloid Interf. Sci. 441 (2015) 1-9.

[23] D.V. Ta, A. Dunn, T.J. Wasley, R.W. Kay, J. Stringer, P.J. Smith, C. Connaughton, J.D. Shephard, Nanosecond laser textured superhydrophobic metallic surfaces and their chemical sensing applications, Appl. Surf. Sci. 357 (2015) 248-254.

[24] L.B. Boinovich, A.M. Emelyanenko, K.A. Emelyanenko, A.G. Domantovsky, A.A. Shiryaev, Comment on “Nanosecond laser textured superhydrophobic metallic surfaces and their chemical sensing applications” by Duong V. Ta, Andrew Dunn, Thomas J. Wasley, Robert W. Kay, Jonathan Stringer, Patrick J. Smith, Colm Connaughton, Jonathan D. Shephard (Appl. Surf. Sci. 357 (2015) 248-254), Appl. Surf. Sci. 379 (2016) 111-113.

[25] J. Long, M. Zhong, P. Fan, D. Gong, H. Zhang, Wettability conversion of ultrafast laser structured copper surface, J. Laser Appl. 27 (2015) S29107.

[26] R.N. Wenzel, Resistance of solid surfaces to wetting by water, J. Ind. Eng. Chem. 28 (1936) 988-994.

[27] A.B.D. Cassie, S. Baxter, Wettability of porous surfaces, Trans. Faraday Soc. 40

(1944) 546-551.

[28] J.T. Cardoso, A. Garcia-Girón, J.M. Romano, D. Huerta-Murillo, R. Jagdheesh, M. Walker, S.S. Dimov, J.L. Ocaña, Influence of ambient conditions on the evolution of wettability properties of an IR-, ns-laser textured aluminium alloy, RSC Adv. 7 (2017) 39617-39627.

[29] J.L. Yong, J.L. Huo, Q. Yang, F. Chen, Y. Fang, X.J. Wu, L. Liu, X.Y. Lu, J.Z. Zhang, X. Hou, Femtosecond laser direct writing of porous network microstructures for the fabricating super-slippery surface with excellent liquid repellence and anti-cell proliferation, Adv. Mater. Interfaces, 5 (2018) 1701479.

[30] E. Dabek-Zlotorzynska, V. Celo, in *capillary electrophoresis: methods and protocols*, ed. P. Schmitt-Kopplin, Humana Press, Totowa, NJ, (2008) 43-64.

[31] J. Drzymala, Hydrophobicity and collectorless flotation of inorganic materials, Adv. Colloid Interfac. 50 (1994) 143-185.

[32] K.C. Hass, W.F. Schneider, A. Curioni, W. Andreoni, The chemistry of water on alumina surfaces: reaction dynamics from first principles, Science 282(1998) 265-268.

[33] D. Argyris, P.D. Ashby, A. Striolo, Structure and orientation of interfacial water determine atomic force microscopy results: insights from molecular dynamics simulations, ACS Nano 5 (2011) 2215-2223.

[34] P. Liu, L. Cao, W. Zhao, Y. Xia, W. Huang, Z.L. Li, Insights into the superhydrophobicity of metallic surfaces prepared by electrodeposition involving spontaneous adsorption of airborne hydrocarbons, Appl. Surf. Sci. 324 (2015) 576-583.

[35] G.P. López, D.G. Castner, B.D. Ratner, XPS O 1s binding energies for polymers containing hydroxyl, ether, ketone and ester groups, Surf. Interface Anal. 17 (1991) 267-272.

[36] A. He, W.W. Liu, W. Xue, H. Yang, Y. Cao, Nanosecond laser ablated copper superhydrophobic surface with tunable ultrahigh adhesion and its renewability with low temperature annealing, Appl. Surf. Sci. 434 (2018) 120-125.

[37] Z.T. Li, Y.J. Wang, A. Kozbial, *et al*, Effect of airborne contaminants on the

wettability of supported graphene and graphite, Nat. Mater. 12 (2013) 925-931.